Search for events with leptonic jets and missing transverse energy in ppbar collisions at sqrt(s)=1.96 TeV

V.M. Abazov, B. Abbott, M. Abolins, B.S. Acharya, M. Adams, T. Adams, G.D. Alexeev, G. Alkhazov, A. Alton, G. Alverson, et al.

FERMILAB-PUB-10-320-E

Search for events with leptonic jets and missing transverse energy in $p\bar{p}$ collisions at $\sqrt{s} = 1.96$ TeV

V.M. Abazov,[35] B. Abbott,[73] M. Abolins,[62] B.S. Acharya,[29] M. Adams,[48] T. Adams,[46] G.D. Alexeev,[35] G. Alkhazov,[39] A. Alton[a],[61] G. Alverson,[60] G.A. Alves,[2] L.S. Ancu,[34] M. Aoki,[47] Y. Arnoud,[14] M. Arov,[57] A. Askew,[46] B. Åsman,[40] O. Atramentov,[65] C. Avila,[8] J. BackusMayes,[80] F. Badaud,[13] L. Bagby,[47] B. Baldin,[47] D.V. Bandurin,[46] S. Banerjee,[29] E. Barberis,[60] P. Baringer,[55] J. Barreto,[2] J.F. Bartlett,[47] U. Bassler,[18] S. Beale,[6] A. Bean,[55] M. Begalli,[3] M. Begel,[71] C. Belanger-Champagne,[40] L. Bellantoni,[47] J.A. Benitez,[62] S.B. Beri,[27] G. Bernardi,[17] R. Bernhard,[22] I. Bertram,[41] M. Besançon,[18] R. Beuselinck,[42] V.A. Bezzubov,[38] P.C. Bhat,[47] V. Bhatnagar,[27] G. Blazey,[49] S. Blessing,[46] K. Bloom,[64] A. Boehnlein,[47] D. Boline,[70] T.A. Bolton,[56] E.E. Boos,[37] G. Borissov,[41] T. Bose,[59] A. Brandt,[76] O. Brandt,[23] R. Brock,[62] G. Brooijmans,[68] A. Bross,[47] D. Brown,[17] J. Brown,[17] X.B. Bu,[7] D. Buchholz,[50] M. Buehler,[79] V. Buescher,[24] V. Bunichev,[37] S. Burdin[b],[41] T.H. Burnett,[80] C.P. Buszello,[42] B. Calpas,[15] S. Calvet,[16] E. Camacho-Pérez,[32] M.A. Carrasco-Lizarraga,[32] E. Carrera,[46] B.C.K. Casey,[47] H. Castilla-Valdez,[32] S. Chakrabarti,[70] D. Chakraborty,[49] K.M. Chan,[53] A. Chandra,[78] G. Chen,[55] S. Chevalier-Théry,[18] D.K. Cho,[75] S.W. Cho,[31] S. Choi,[31] B. Choudhary,[28] T. Christoudias,[42] S. Cihangir,[47] D. Claes,[64] J. Clutter,[55] M. Cooke,[47] W.E. Cooper,[47] M. Corcoran,[78] F. Couderc,[18] M.-C. Cousinou,[15] A. Croc,[18] D. Cutts,[75] M. Ćwiok,[30] A. Das,[44] G. Davies,[42] K. De,[76] S.J. de Jong,[34] E. De La Cruz-Burelo,[32] F. Déliot,[18] D. DeMair,[65] M. Demarteau,[47] R. Demina,[69] D. Denisov,[47] S.P. Denisov,[38] S. Desai,[47] K. DeVaughan,[64] H.T. Diehl,[47] M. Diesburg,[47] A. Dominguez,[64] T. Dorland,[80] A. Dubey,[28] L.V. Dudko,[37] D. Duggan,[65] A. Duperrin,[15] S. Dutt,[27] A. Dyshkant,[49] M. Eads,[64] D. Edmunds,[62] J. Ellison,[45] V.D. Elvira,[47] Y. Enari,[17] S. Eno,[58] H. Evans,[51] A. Evdokimov,[71] V.N. Evdokimov,[38] G. Facini,[60] A.V. Ferapontov,[75] T. Ferbel,[58,69] F. Fiedler,[24] F. Filthaut,[34] W. Fisher,[62] H.E. Fisk,[47] M. Fortner,[49] H. Fox,[41] S. Fuess,[47] T. Gadfort,[71] A. Garcia-Bellido,[69] V. Gavrilov,[36] P. Gay,[13] W. Geist,[19] W. Geng,[15,62] D. Gerbaudo,[66] C.E. Gerber,[48] Y. Gershtein,[65] G. Ginther,[47,69] G. Golovanov,[35] A. Goussiou,[80] P.D. Grannis,[70] S. Greder,[19] H. Greenlee,[47] Z.D. Greenwood,[57] E.M. Gregores,[4] G. Grenier,[20] Ph. Gris,[13] J.-F. Grivaz,[16] A. Grohsjean,[18] S. Grünendahl,[47] M.W. Grünewald,[30] F. Guo,[70] J. Guo,[70] G. Gutierrez,[47] P. Gutierrez,[73] A. Haas[c],[68] S. Hagopian,[46] J. Haley,[60] L. Han,[7] K. Harder,[43] A. Harel,[69] J.M. Hauptman,[54] J. Hays,[42] T. Hebbeker,[21] D. Hedin,[49] H. Hegab,[74] A.P. Heinson,[45] U. Heintz,[75] C. Hensel,[23] I. Heredia-De La Cruz,[32] K. Herner,[61] G. Hesketh,[60] M.D. Hildreth,[53] R. Hirosky,[79] T. Hoang,[46] J.D. Hobbs,[70] B. Hoeneisen,[12] M. Hohlfeld,[24] S. Hossain,[73] Z. Hubacek,[10] N. Huske,[17] V. Hynek,[10] I. Iashvili,[67] R. Illingworth,[47] A.S. Ito,[47] S. Jabeen,[75] M. Jaffré,[16] S. Jain,[67] D. Jamin,[15] R. Jesik,[42] K. Johns,[44] M. Johnson,[47] D. Johnston,[64] A. Jonckheere,[47] P. Jonsson,[42] J. Joshi,[27] A. Juste[d],[47] K. Kaadze,[56] E. Kajfasz,[15] D. Karmanov,[37] P.A. Kasper,[47] I. Katsanos,[64] R. Kehoe,[77] S. Kermiche,[15] N. Khalatyan,[47] A. Khanov,[74] A. Kharchilava,[67] Y.N. Kharzheev,[35] D. Khatidze,[75] M.H. Kirby,[50] J.M. Kohli,[27] A.V. Kozelov,[38] J. Kraus,[62] A. Kumar,[67] A. Kupco,[11] T. Kurča,[20] V.A. Kuzmin,[37] J. Kvita,[9] S. Lammers,[51] G. Landsberg,[75] P. Lebrun,[20] H.S. Lee,[31] S.W. Lee,[54] W.M. Lee,[47] J. Lellouch,[17] L. Li,[45] Q.Z. Li,[47] S.M. Lietti,[5] J.K. Lim,[31] D. Lincoln,[47] J. Linnemann,[62] V.V. Lipaev,[38] R. Lipton,[47] Y. Liu,[7] Z. Liu,[6] A. Lobodenko,[39] M. Lokajicek,[11] P. Love,[41] H.J. Lubatti,[80] R. Luna-Garcia[e],[32] A.L. Lyon,[47] A.K.A. Maciel,[2] D. Mackin,[78] R. Madar,[18] R. Magaña-Villalba,[32] S. Malik,[64] V.L. Malyshev,[35] Y. Maravin,[56] J. Martínez-Ortega,[32] R. McCarthy,[70] C.L. McGivern,[55] M.M. Meijer,[34] A. Melnitchouk,[63] D. Menezes,[49] P.G. Mercadante,[4] M. Merkin,[37] A. Meyer,[21] J. Meyer,[23] N.K. Mondal,[29] G.S. Muanza,[15] M. Mulhearn,[79] E. Nagy,[15] M. Naimuddin,[28] M. Narain,[75] R. Nayyar,[28] H.A. Neal,[61] J.P. Negret,[8] P. Neustroev,[39] H. Nilsen,[22] S.F. Novaes,[5] T. Nunnemann,[25] G. Obrant,[39] D. Onoprienko,[56] J. Orduna,[32] N. Osman,[42] J. Osta,[53] G.J. Otero y Garzón,[1] M. Owen,[43] M. Padilla,[45] M. Pangilinan,[75] N. Parashar,[52] V. Parihar,[75] S.K. Park,[31] J. Parsons,[68] R. Partridge[c],[75] N. Parua,[51] A. Patwa,[71] B. Penning,[47] M. Perfilov,[37] K. Peters,[43] Y. Peters,[43] G. Petrillo,[69] P. Pétroff,[16] R. Piegaia,[1] J. Piper,[62] M.-A. Pleier,[71] P.L.M. Podesta-Lerma[f],[32] V.M. Podstavkov,[47] M.-E. Pol,[2] P. Polozov,[36] A.V. Popov,[38] M. Prewitt,[78] D. Price,[51] S. Protopopescu,[71] J. Qian,[61] A. Quadt,[23] B. Quinn,[63] M.S. Rangel,[16] K. Ranjan,[28] P.N. Ratoff,[41] I. Razumov,[38] P. Renkel,[77] P. Rich,[43] M. Rijssenbeek,[70] I. Ripp-Baudot,[19] F. Rizatdinova,[74] M. Rominsky,[47] C. Royon,[18] P. Rubinov,[47] R. Ruchti,[53] G. Safronov,[36] G. Sajot,[14] A. Sánchez-Hernández,[32] M.P. Sanders,[25] B. Sanghi,[47] A.S. Santos,[5]

G. Savage,[47] L. Sawyer,[57] T. Scanlon,[42] R.D. Schamberger,[70] Y. Scheglov,[39] H. Schellman,[50] T. Schliephake,[26] S. Schlobohm,[80] C. Schwanenberger,[43] R. Schwienhorst,[62] J. Sekaric,[55] H. Severini,[73] E. Shabalina,[23] V. Shary,[18] A.A. Shchukin,[38] R.K. Shivpuri,[28] V. Simak,[10] V. Sirotenko,[47] P. Skubic,[73] P. Slattery,[69] D. Smirnov,[53] K.J. Smith,[67] G.R. Snow,[64] J. Snow,[72] S. Snyder,[71] S. Söldner-Rembold,[43] L. Sonnenschein,[21] A. Sopczak,[41] M. Sosebee,[76] K. Soustruznik,[9] B. Spurlock,[76] J. Stark,[14] V. Stolin,[36] D.A. Stoyanova,[38] E. Strauss,[70] M. Strauss,[73] D. Strom,[48] L. Stutte,[47] P. Svoisky,[34] M. Takahashi,[43] A. Tanasijczuk,[1] W. Taylor,[6] M. Titov,[18] V.V. Tokmenin,[35] D. Tsybychev,[70] B. Tuchming,[18] C. Tully,[66] P.M. Tuts,[68] L. Uvarov,[39] S. Uvarov,[39] S. Uzunyan,[49] R. Van Kooten,[51] W.M. van Leeuwen,[33] N. Varelas,[48] E.W. Varnes,[44] I.A. Vasilyev,[38] P. Verdier,[20] L.S. Vertogradov,[35] M. Verzocchi,[47] M. Vesterinen,[43] D. Vilanova,[18] P. Vint,[42] P. Vokac,[10] H.D. Wahl,[46] M.H.L.S. Wang,[69] J. Warchol,[53] G. Watts,[80] M. Wayne,[53] M. Weber[g],[47] M. Wetstein,[58] A. White,[76] D. Wicke,[24] M.R.J. Williams,[41] G.W. Wilson,[55] S.J. Wimpenny,[45] M. Wobisch,[57] D.R. Wood,[60] T.R. Wyatt,[43] Y. Xie,[47] C. Xu,[61] S. Yacoob,[50] R. Yamada,[47] W.-C. Yang,[43] T. Yasuda,[47] Y.A. Yatsunenko,[35] Z. Ye,[47] H. Yin,[7] K. Yip,[71] H.D. Yoo,[75] S.W. Youn,[47] J. Yu,[76] S. Zelitch,[79] T. Zhao,[80] B. Zhou,[61] J. Zhu,[61] M. Zielinski,[69] D. Zieminska,[51] and L. Zivkovic[68]

(The D0 Collaboration*)

[1]*Universidad de Buenos Aires, Buenos Aires, Argentina*
[2]*LAFEX, Centro Brasileiro de Pesquisas Físicas, Rio de Janeiro, Brazil*
[3]*Universidade do Estado do Rio de Janeiro, Rio de Janeiro, Brazil*
[4]*Universidade Federal do ABC, Santo André, Brazil*
[5]*Instituto de Física Teórica, Universidade Estadual Paulista, São Paulo, Brazil*
[6]*Simon Fraser University, Vancouver, British Columbia, and York University, Toronto, Ontario, Canada*
[7]*University of Science and Technology of China, Hefei, People's Republic of China*
[8]*Universidad de los Andes, Bogotá, Colombia*
[9]*Charles University, Faculty of Mathematics and Physics, Center for Particle Physics, Prague, Czech Republic*
[10]*Czech Technical University in Prague, Prague, Czech Republic*
[11]*Center for Particle Physics, Institute of Physics, Academy of Sciences of the Czech Republic, Prague, Czech Republic*
[12]*Universidad San Francisco de Quito, Quito, Ecuador*
[13]*LPC, Université Blaise Pascal, CNRS/IN2P3, Clermont, France*
[14]*LPSC, Université Joseph Fourier Grenoble 1, CNRS/IN2P3, Institut National Polytechnique de Grenoble, Grenoble, France*
[15]*CPPM, Aix-Marseille Université, CNRS/IN2P3, Marseille, France*
[16]*LAL, Université Paris-Sud, CNRS/IN2P3, Orsay, France*
[17]*LPNHE, Universités Paris VI and VII, CNRS/IN2P3, Paris, France*
[18]*CEA, Irfu, SPP, Saclay, France*
[19]*IPHC, Université de Strasbourg, CNRS/IN2P3, Strasbourg, France*
[20]*IPNL, Université Lyon 1, CNRS/IN2P3, Villeurbanne, France and Université de Lyon, Lyon, France*
[21]*III. Physikalisches Institut A, RWTH Aachen University, Aachen, Germany*
[22]*Physikalisches Institut, Universität Freiburg, Freiburg, Germany*
[23]*II. Physikalisches Institut, Georg-August-Universität Göttingen, Göttingen, Germany*
[24]*Institut für Physik, Universität Mainz, Mainz, Germany*
[25]*Ludwig-Maximilians-Universität München, München, Germany*
[26]*Fachbereich Physik, Bergische Universität Wuppertal, Wuppertal, Germany*
[27]*Panjab University, Chandigarh, India*
[28]*Delhi University, Delhi, India*
[29]*Tata Institute of Fundamental Research, Mumbai, India*
[30]*University College Dublin, Dublin, Ireland*
[31]*Korea Detector Laboratory, Korea University, Seoul, Korea*
[32]*CINVESTAV, Mexico City, Mexico*
[33]*FOM-Institute NIKHEF and University of Amsterdam/NIKHEF, Amsterdam, The Netherlands*
[34]*Radboud University Nijmegen/NIKHEF, Nijmegen, The Netherlands*
[35]*Joint Institute for Nuclear Research, Dubna, Russia*
[36]*Institute for Theoretical and Experimental Physics, Moscow, Russia*
[37]*Moscow State University, Moscow, Russia*
[38]*Institute for High Energy Physics, Protvino, Russia*
[39]*Petersburg Nuclear Physics Institute, St. Petersburg, Russia*
[40]*Stockholm University, Stockholm and Uppsala University, Uppsala, Sweden*
[41]*Lancaster University, Lancaster LA1 4YB, United Kingdom*
[42]*Imperial College London, London SW7 2AZ, United Kingdom*
[43]*The University of Manchester, Manchester M13 9PL, United Kingdom*

[44] *University of Arizona, Tucson, Arizona 85721, USA*
[45] *University of California Riverside, Riverside, California 92521, USA*
[46] *Florida State University, Tallahassee, Florida 32306, USA*
[47] *Fermi National Accelerator Laboratory, Batavia, Illinois 60510, USA*
[48] *University of Illinois at Chicago, Chicago, Illinois 60607, USA*
[49] *Northern Illinois University, DeKalb, Illinois 60115, USA*
[50] *Northwestern University, Evanston, Illinois 60208, USA*
[51] *Indiana University, Bloomington, Indiana 47405, USA*
[52] *Purdue University Calumet, Hammond, Indiana 46323, USA*
[53] *University of Notre Dame, Notre Dame, Indiana 46556, USA*
[54] *Iowa State University, Ames, Iowa 50011, USA*
[55] *University of Kansas, Lawrence, Kansas 66045, USA*
[56] *Kansas State University, Manhattan, Kansas 66506, USA*
[57] *Louisiana Tech University, Ruston, Louisiana 71272, USA*
[58] *University of Maryland, College Park, Maryland 20742, USA*
[59] *Boston University, Boston, Massachusetts 02215, USA*
[60] *Northeastern University, Boston, Massachusetts 02115, USA*
[61] *University of Michigan, Ann Arbor, Michigan 48109, USA*
[62] *Michigan State University, East Lansing, Michigan 48824, USA*
[63] *University of Mississippi, University, Mississippi 38677, USA*
[64] *University of Nebraska, Lincoln, Nebraska 68588, USA*
[65] *Rutgers University, Piscataway, New Jersey 08855, USA*
[66] *Princeton University, Princeton, New Jersey 08544, USA*
[67] *State University of New York, Buffalo, New York 14260, USA*
[68] *Columbia University, New York, New York 10027, USA*
[69] *University of Rochester, Rochester, New York 14627, USA*
[70] *State University of New York, Stony Brook, New York 11794, USA*
[71] *Brookhaven National Laboratory, Upton, New York 11973, USA*
[72] *Langston University, Langston, Oklahoma 73050, USA*
[73] *University of Oklahoma, Norman, Oklahoma 73019, USA*
[74] *Oklahoma State University, Stillwater, Oklahoma 74078, USA*
[75] *Brown University, Providence, Rhode Island 02912, USA*
[76] *University of Texas, Arlington, Texas 76019, USA*
[77] *Southern Methodist University, Dallas, Texas 75275, USA*
[78] *Rice University, Houston, Texas 77005, USA*
[79] *University of Virginia, Charlottesville, Virginia 22901, USA*
[80] *University of Washington, Seattle, Washington 98195, USA*

(Dated: August 19, 2010)

We present the first search for pair production of isolated jets of charged leptons in association with a large imbalance in transverse energy in $p\bar{p}$ collisions using 5.8 fb^{-1} of integrated luminosity collected by the D0 detector at the Fermilab Tevatron Collider. No excess is observed above Standard Model background, and the result is used to set upper limits on the production cross section of pairs of supersymmetric chargino and neutralino particles as a function of "dark-photon" mass, where the dark photon is produced in the decay of the lightest supersymmetric particle.

PACS numbers: 12.60.Jv, 14.80.Ly

Hidden-valley models [1] contain a hidden sector that is very weakly coupled to standard-model (SM) particles. By introducing new low-mass particles in the hidden sector, these models have been shown to provide cogent interpretation [2, 3] of possible astrophysical anomalies [4, 5, 6], and accommodate discrepancies in direct searches for dark matter [7, 8]. The impact of the hidden valley particles should be observable in high-energy collisions [9, 10, 11, 12]. Although details of the hidden sector can affect the phenomenology, the force carrier in the hidden sector, the dark-photon (γ_D), must have a mass $\lesssim$ 2 GeV, and generally decays into SM charged-fermion (or pion) pairs. In many models, γ_D has a short lifetime, and does not travel an observable distance ($\lesssim 1$ μm) before decaying. If supersymmetry (SUSY) is realized in Nature, there will be partners for both the SM and the hidden sector particles. If the lightest SUSY particle (LSP) of the hidden sector ($\tilde{X}$) is lighter than the lightest SM SUSY partner (SM-LSP), the SM-LSP can decay

*with visitors from [a]Augustana College, Sioux Falls, SD, USA, [b]The University of Liverpool, Liverpool, UK, [c]SLAC, Menlo Park, CA, USA, [d]ICREA/IFAE, Barcelona, Spain, [e]Centro de Investigacion en Computacion - IPN, Mexico City, Mexico, [f]ECFM, Universidad Autonoma de Sinaloa, Culiacán, Mexico, and [g]Universität Bern, Bern, Switzerland.

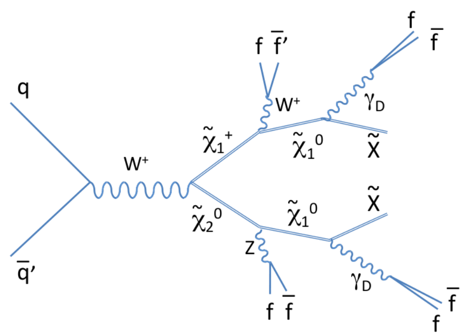

FIG. 1: A diagram for associated production of SUSY charginos and neutralinos that decay into SM vector bosons and SM-LSPs ($\tilde{X}_1^0$), each decaying into the LSP of the hidden-sector ($\tilde{X}$) and a dark-photon (γ_D).

promptly into particles of the hidden sector, and always will do so if R-parity is conserved. The D0 collaboration has reported [13] a search for such a decay, with one SM-LSP decaying to a SM photon and $\tilde{X}$, and the other to γ_D and $\tilde{X}$. However, the SM-LSP might decay predominantly into hidden sector particles, thereby yielding two or more γ_D in each event, as indicated in Fig. 1. Pair-produced dark photons could also arise from rare decays of Z bosons [9, 14] and Higgs bosons [12]. Single dark photons should also be produced directly in association with a jet, as in SM prompt-photon production. This process is difficult to detect at a hadron collider, while high-luminosity low-energy e^+e^- colliders could be more effective in observing such events [15, 16].

Since hidden-sector particles have small mass and they are produced with high velocities, their decays through the hidden sector can produce jets of tightly collimated particles from decays of γ_D. If $M(\gamma_D) < 2m(\pi)$, the jets will consist only of charged leptons. Even for larger $M(\gamma_D)$, the lepton content of these jets will be high, and we therefore refer to them as leptonic jets (l-jets). For the proposed scenario, every SUSY event will have at least two l-jets and a large imbalance in transverse energy ($\not{E}_T$) from the escaping $\tilde{X}$ and possibly also from other escaping dark particles. Radiation of additional γ_D in the hidden sector [9] can dilute the l-jet signatures, by producing final-state particles in l-jets that are softer, less tightly collimated, and less isolated.

In this Letter, we present a search for events with two l-jets and large $\not{E}_T$ in data collected using the D0 [17] detector during Run II of the Fermilab Tevatron Collider, corresponding to an integrated luminosity of 5.8 fb^{-1}. Depending on whether the γ_D decays to muons or electrons, the l-jet can appear either as a "muon l-jet" or an "electron l-jet" in the detector. To reconstruct muon l-jets, we demand a muon-track candidate with hits in all three layers of the outer D0 muon system and a matching track with $p_T > 10$ GeV in the central tracker. An electron l-jet must contain a central track with $p_T > 10$ GeV that matches an electromagnetic (EM) calorimeter cluster with transverse energy $E_T^{\rm EM}$ >15 GeV within a cone of radius $\mathcal{R} = \sqrt{(\Delta\eta)^2 + (\Delta\phi)^2} < 0.2$ [18]. EM clusters are formed using a simple cone algorithm of $\mathcal{R} = 0.4$ and require $> 95\%$ of the energy to be deposited in the EM section of the calorimeter. The calorimeter isolation variable $\mathcal{I}_e = [E_T^{\rm tot}(0.4) - E_T^{\rm EM}(0.2)]/E_T^{\rm EM}(0.2)$ must be $\mathcal{I}_e < 0.2$, where $E_T^{\rm tot}(0.4)$ is the total transverse energy in a cone of radius $\mathcal{R} = 0.4$, corrected for contributions from the underlying event, and $E_T^{\rm EM}(0.2)$ is the transverse EM energy in a cone of radius $\mathcal{R} = 0.2$. The central "seed" track matched to the muon or EM cluster is required to have at least one hit in the silicon detector. When the seed track is matched to both a muon and an EM cluster, the l-jet is defined as a muon l-jet. Next, a companion track of opposite electric charge from the seed track, and within $z = 1$ cm of the seed track at its distance of closest approach to the beamline, is required to have $p_T > 4$ GeV and be within $\mathcal{R} < 0.2$ of the seed track. If more than one such companion track is found, we use the one with smallest $\mathcal{R}$. No explicit requirements are made on the distances of closest approach of tracks to the collision point, thus the l-jet reconstruction efficiency remains high for γ_D decay radii up to ≈ 1 cm. We then choose the pair of l-jet candidates with seed tracks separated by $\mathcal{R} > 0.8$ that have the largest invariant mass of any pair of seed tracks in the event.

The MadGraph [19] MC event generator, with PYTHIA [20] for showering and hadronization, is used to simulate the signal, and these Monte Carlo (MC) events are then processed through the full GEANT3-based [21] D0-detector simulation and event reconstruction software. SUSY events generated using SPS8 [22] parameters of the gauge-mediated-SUSY-breaking (GMSB) model are used as a benchmark. The efficiency to reconstruct many tightly-collimated tracks is difficult to determine from data, and we therefore assume that all neutralinos decay directly into a single γ_D and the dark gaugino LSP $\tilde{X}$, giving just two leptons per l-jet. The $\tilde{X}$ would, most naturally, have a similar mass as γ_D, so we assume $m(\tilde{X}) = 1$ GeV. More complicated hidden-sector options are studied using MC simulation and are discussed below.

The analysis requires two l-jet candidates (either muon or electron) in each event. The three classes of $\mu\mu$, $e\mu$, and ee l-jets are analyzed separately, and contain 7344, 19014, and 30642 candidate events, respectively. Each event is assigned to just one class, with preference of choice given to $\mu\mu$, then $e\mu$, and then ee, since muon l-jets have less background. All collected events are used in the analysis, but most pass single or di-lepton triggers [17]. Following offline selections, the trigger efficiency for signal is $> 90\%$.

The main background to l-jets is from multijet production, but electron l-jets also have a contribution

TABLE I: The ratio $\mathcal{R}_{\not{f}}$ of events with two l-jets and $\not\!\!E_T > 30$ GeV divided by the number with $\not\!\!E_T < 15$ GeV in the non-isolated data sample (see text); events observed and predicted from background in each channel; the acceptance of the chosen SPS8 [22] SUSY MC point, and the reconstruction efficiency, given in %; branching ratios ($\mathcal{B}$) for each channel, calculated from $\mathcal{B}_e$ and $\mathcal{B}_\mu$ in Table II. Finally, limits on cross sections times $\mathcal{B}$ from the inclusive l-jet search.

Chan.	$\mathcal{R}_{\not{f}}$	$N_{\rm obs}$	$N_{\rm pred}$	$\mathcal{A}(\%)$	$\epsilon(\%)$	$\mathcal{B}$	$\sigma_{95\%} \times \mathcal{B}$, fb obs.	$\sigma_{95\%} \times \mathcal{B}$, fb pred.
$\mu\mu$	0.33	3	8.6±4.5	50	12	$\mathcal{B}_\mu^2$	20	35^{+26}_{-21}
$e\mu$	0.37	11	17.5±4.2	53	15	$2\mathcal{B}_e\mathcal{B}_\mu$	19	30^{+19}_{-15}
ee	0.04	7	10.2±1.7	45	20	$\mathcal{B}_e^2$	13	19^{+11}_{-9}

from photon production with subsequent conversion to e^+e^-. Such backgrounds cannot be calculated reliably using simulation, and are therefore determined from data. We exploit the tight collimation of l-jets to distinguish them from multijet background, through track and calorimeter-isolation criteria. The "track isolation" is defined by a scalar sum over p_T of tracks with $p_T > 0.5$ GeV, $z < 1$ cm from the seed track at its distance of closest approach to the beamline, and within an annulus $0.2 < \mathcal{R} < 0.4$ relative to the seed track. Muon l-jet calorimeter isolation ($\mathcal{I}_\mu$), defined in Ref. [23], relies on the transverse energies of all calorimeter cells within $\mathcal{R} < 0.4$, excluding cells within $\mathcal{R} < 0.1$ of either the seed muon or its companion track. For electron l-jet isolation, we employ the EM cluster-isolation $\mathcal{I}_e$ defined above. A reliable estimate of background requires that the l-jet isolation requirements not bias the kinematics, such as distributions in $\not\!\!E_T$ or p_T of l-jets. Both types of l-jets require the track isolation to be $\mathcal{I}_l < 2$ GeV, which does not significantly bias the background. Calorimeter-isolation criteria are chosen as linear functions of p_T values of the l-jet, such that the fraction of rejected background is large, but weakly dependent on $\not\!\!E_T$, as discussed below. For EM clusters, we choose $\mathcal{I}_e < 0.085 \times p_T - 0.53$ (in GeV units), which rejects 90% of the background. For muon l-jets we use the scalar sum of p_T values of the muon and companion tracks as a measure of l-jet p_T, and require $\mathcal{I}_\mu < 0.066 \times p_T + 2.35$ (in GeV units), which rejects 94% of the background. We compare the $\not\!\!E_T$ distribution in data with just one isolated l-jet to those containing two (not necessarily isolated) l-jets. The two distributions are observed to be very similar, which indicates that the kinematic bias on $\not\!\!E_T$ from $\mathcal{I}_e$ and $\mathcal{I}_\mu$ requirements is indeed small. We therefore use the $\not\!\!E_T$ distribution in data without isolation requirements as background for the data with two isolated l-jets, since both samples are dominated by similar multijet processes.

Finally, we require $\not\!\!E_T > 30$ GeV for the search sample, where $\not\!\!E_T$ is calculated using only calorimetric information, and not corrected for any detected muons, as muon

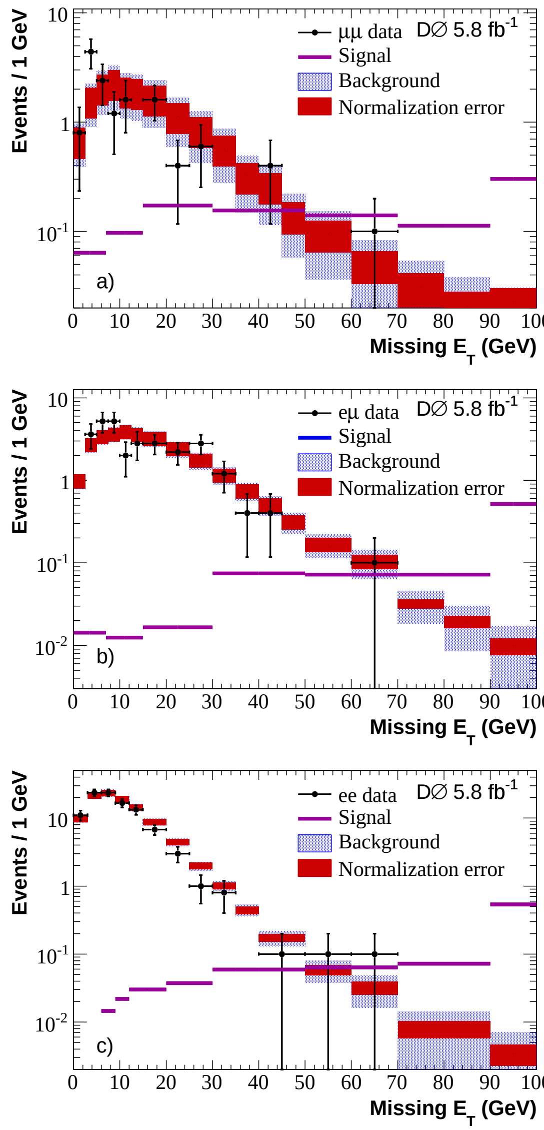

FIG. 2: (color online) The $\not\!\!E_T$ distribution for events with (a) two isolated muon l-jets, (b) one muon and one electron l-jet, and (c) two electron l-jets. The data are presented by the black points, and the shaded bands represent the expected background, with red showing the correlated part of the systematic uncertainty from normalization and blue the full uncertainty. The SPS8 MC contribution for signal (see text) is scaled to an integrated content of 10 events. The highest bin contains all events with $\not\!\!E_T > 90$ GeV.

reconstruction is unreliable in l-jets because of the presence of nearby tracks. We scale the $\not\!\!E_T$ distribution in the data sample without isolation criteria so that the total number of events with $\not\!\!E_T < 15$ GeV matches that in the isolated data sample, see Fig. 2. The ratio $\mathcal{R}_{\not{f}}$ defined as the number of events in each search channel with $\not\!\!E_T > 30$ GeV divided by the scaled number of events with $\not\!\!E_T < 15$ GeV in each respective background is given in Table I. The value of $\mathcal{R}_{\not{f}}$ is important since if a signal

TABLE II: Branching ratio ($\mathcal{B}$) into electrons and muons of γ_D as a function of its mass. Mass windows for a search for γ_D, and the efficiency for a reconstructed, isolated l-jet to be found in each mass window, for electron and muon l-jets.

$M(\gamma_D)$ (GeV)	$\mathcal{B}_e/\mathcal{B}_\mu$	$\Delta M(l\text{-jet})$(GeV)	Eff. $ee/\mu\mu$(%)
0.15	1.00/0.00	0.0–0.3	81/–
0.3	0.53/0.47	0.1–0.4	82/88
0.5	0.40/0.40	0.3–0.6	81/89
0.7	0.15/0.15	0.4–0.8	85/89
0.9	0.27/0.27	0.6–1.1	82/91
1.3	0.31/0.31	0.9–1.4	72/79
1.7	0.22/0.22	1.0–1.8	73/76
2.0	0.24/0.24	1.3–2.2	73/83

has a $\not\!\!E_T$ spectrum similar to that of the background, this analysis would be largely insensitive, regardless of the size of the signal. The total background for a signal having f_1 events with $\not\!\!E_T < 15$ GeV and f_2 events with $\not\!\!E_T > 30$ GeV is a factor of $(f_1/f_2) \times \mathcal{R}_{\not f}$ larger than for the case of no signal. For the benchmark signals considered, $(f_1/f_2) \times \mathcal{R}_{\not f} \ll 1$, and the correction is therefore ignored.

We separate the detection efficiency into three components (Table I): (i) the branching ratio ($\mathcal{B}$) for an event to have at least two l-jets in the $\mu\mu$, $e\mu$, or ee channel, obtained from the expected γ_D branching fractions [13], (ii) the acceptance ($\mathcal{A}$) for both l-jets to have the seed and companion tracks within $|\eta| < 1.1$ for electrons and < 1.6 for muons, with $p_T > 10$ and 4 GeV, respectively, and $\not\!\!E_T$ (calculated in MC as the vector sum of transverse momenta of all stable particles in the hidden sector, neutrinos, and muons) > 30 GeV, and (iii) the efficiency (ϵ) to reconstruct both l-jets in the acceptance, to pass the isolation criteria for both l-jets, and to have reconstructed $\not\!\!E_T$ in excess of 30 GeV. The acceptance and reconstruction efficiency do not vary significantly with $M(\gamma_D)$.

With no excess observed above the expected background at large $\not\!\!E_T$ (see Fig. 2), we set limits on l-jet production cross sections, using a likelihood fitter [24] that incorporates a log-likelihood ratio statistic [25]. Limits at the 95% CL on cross section times $\mathcal{B}$, calculated separately for the $\mu\mu$, $e\mu$, and ee channels, using the observed numbers of events, predicted backgrounds, and detection efficiencies and acceptances, are given in Table I. Systematic uncertainties are included for signal efficiency (20%), background normalization (20-50%), and luminosity (6.1%). The uncertainty on the signal efficiency is dominated by the uncertainty in the tracking efficiency for neighboring tracks in data. The background uncertainty is dominated by the small remaining kinematic bias on the $\not\!\!E_T$ arising from the isolation criteria.

When the track multiplicity in any l-jet is small, the leading track and its companion track are likely to originate from the decay of the same dark photon, so we also examine the invariant mass of the seed and its companion track ($M(\gamma_D)$) in events with two isolated l-jets and $\not\!\!E_T > 30$ GeV (Fig. 3). The backgrounds are normalized by scaling the events passing all selections but with $\not\!\!E_T < 20$ GeV to data with $\not\!\!E_T > 30$ GeV outside of the mass windows defined in Tab. II, thus $\mathcal{R}_{\not f}$ is irrelevant for this second analysis. The selection of background events is loosened to $\not\!\!E_T < 20$ GeV for this resonance search to increase the statistics of the sample. Limits on cross sections are calculated in various ranges of l-jet mass, $\Delta M(l\text{-jet})$, as shown in Tab. II and Fig. 4.

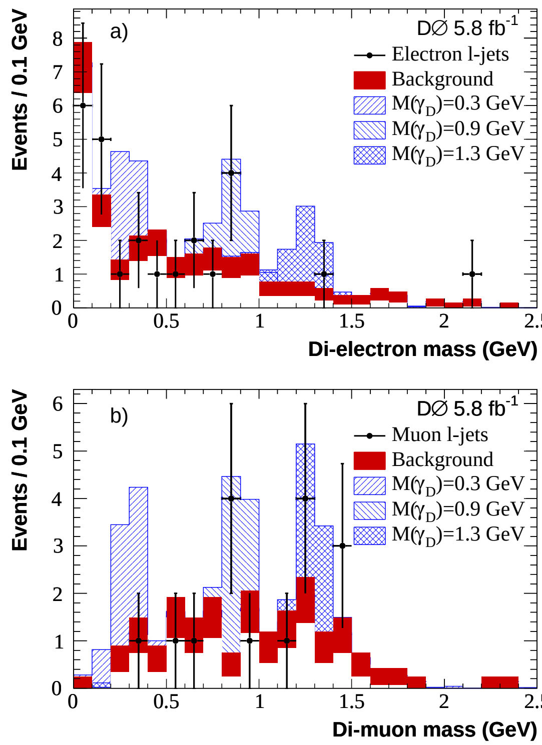

FIG. 3: (color online) Invariant mass of dark photon candidates with two isolated l-jets and $\not\!\!E_T > 30$ GeV, for (a) electron l-jets (in the ee and $e\mu$ channels) and (b) muon l-jets (in the $e\mu$ and $\mu\mu$ channels). Each candidate event contributes two entries, one for each l-jet. The red band shows the mass distribution for events with $\not\!\!E_T < 20$ GeV, normalized to the number of entries with $\not\!\!E_T > 30$ GeV. The shaded blue histograms show the shapes of MC signals added to backgrounds, arbitrarily scaled to an integrated content of 8 signal events, for $M(\gamma_D) = 0.3$, 0.9, and 1.3 GeV.

The dependence of the efficiency for reconstructing and identifying l-jets on parameters of the hidden sector is studied using MC simulation. Additional MC samples are used for examining the neutralino decay into a dark Higgs boson that decays into two dark photons, leading to more, but softer, leptons in l-jets. Efficiency for these states decreases by ≈50% at large $M(\gamma_D)$, for both elec-

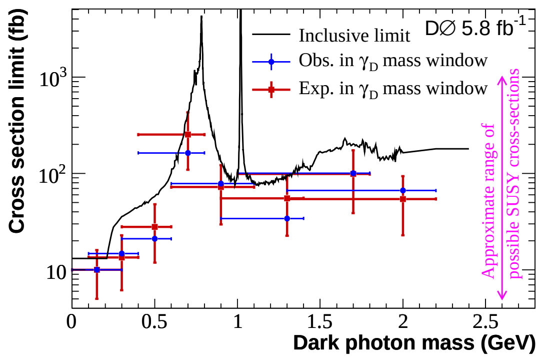

FIG. 4: (color online) Limit on the observed cross section (blue, solid curve) for the three channels combined, corrected for SPS8 acceptance, as a function of $M(\gamma_D)$. Also shown are the observed (blue, circles) and expected (red, squares) combined limit determined using the measured masses of the seed and companion tracks in both l-jets, for each mass window studied (from Table II). Limits are weaker when the dark photon branching ratio to hadrons is larger, particularly near the ρ and ϕ resonances.

tron and muon l-jets. The point $M(\gamma_D) = 0.7$ GeV also has a ≈50% lower efficiency, due to the large branching fraction of γ_D to hadrons. MC events are also generated with additional radiation in the hidden sector. Raising the dark coupling (α_D) from 0 to 0.3 reduces the efficiency by up to 20%, independent of $M(\gamma_D)$. According to MC simulation, the l-jet identification criteria maintain good efficiency even for more complicated behavior in the hidden sector.

In summary, we have performed a search for events with two tightly collimated jets consisting mainly of charged leptons and large $\not\!\!E_T$ in 5.8 fb^{-1} of integrated luminosity. The invariant mass of the l-jets, formed by a seed track and a companion track was also examined for a resonant signal. No evidence was observed for such signals, and upper limits were set, as a function of $M(\gamma_D)$, on the production cross section for SUSY particles decaying to two l-jets and large $\not\!\!E_T$.

We thank A. Falkowski, J. Ruderman, M. Strassler, S. Thomas, I. Yavin, and J. Wacker for many useful discussions and guidance. We thank the staffs at Fermilab and collaborating institutions, and acknowledge support from the DOE and NSF (USA); CEA and CNRS/IN2P3 (France); FASI, Rosatom and RFBR (Russia); CNPq, FAPERJ, FAPESP and FUNDUNESP (Brazil); DAE and DST (India); Colciencias (Colombia); CONACyT (Mexico); KRF and KOSEF (Korea); CONICET and UBACyT (Argentina); FOM (The Netherlands); STFC and the Royal Society (United Kingdom); MSMT and GACR (Czech Republic); CRC Program and NSERC (Canada); BMBF and DFG (Germany); SFI (Ireland); The Swedish Research Council (Sweden); and CAS and CNSF (China).

[1] T. Han *et al.*, J. High Energy Phys. **07**, 008 (2008); M. Strassler and K. Zurek, Phys. Lett. B **651**, 374 (2007).
[2] D.P. Finkbeiner and N. Weiner, Phys. Rev. D **76** 083519 (2007).
[3] N. Arkani-Hamed *et al.*, Phys. Rev. D **79** 015014 (2009).
[4] A.A. Abdo *et al.*, Phys. Rev. Lett. **102**, 181101 (2009).
[5] O. Adriani *et al.*, Nature **458**, 607 (2009).
[6] J. Chang *et al.*, Nature **456**, 362 (2008).
[7] R. Bernabei *et al.* (DAMA/LIBRA Collaboration), Eur. Phys. J. C **56**, 333 (2008).
[8] Z. Ahmed *et al.* (CDMS II Collaboration), Science **327** (5973), 1619 (2010).
[9] M. Baumgart *et al.*, J. High Energy Phys. **04**, 014 (2009).
[10] D.S.M. Alves *et al.*, arXiv:0903.3945 [hep-ph] [Phys. Lett. B (to be published)].
[11] A. Katz and R. Sundrum, J. High Energy Phys. **06**, 003 (2009).
[12] A. Falkowski *et al.*, arXiv:1002.2952 [hep-ph].
[13] V. M. Abazov *et al.* (D0 Collaboration), Phys. Rev. Lett. **103**, 081802, (2009).
[14] C. Cheung *et al.*, J. High Energy Phys. **04**, 116 (2010).
[15] B. Aubert *et al.* (BaBar Collaboration), arXiv:0908.2821; B. Aubert *et al.* (BaBar Collaboration), Phys. Rev. Lett. **103**, 081803 (2009).
[16] J. D. Bjorken *et al.*, Phys. Rev. D **80** 075018 (2009).
[17] V. M. Abazov *et al.* (D0 Collaboration), Nucl. Instrum. Methods Phys. Res. A **565**, 463 (2006).
[18] D0 uses a right-handed coordinate system, with the z-axis pointing in the direction of the proton beam and the y-axis pointing upwards. The azimuthal angle ϕ is defined in the xy plane, and is measured from the x-axis. The pseudorapidity is defined as $\eta = -\ln[\tan(\theta/2)]$, where θ is the polar angle.
[19] J. Alwall *et al.*, J. High Energy Phys. **09**, 028 (2007).
[20] T. Sjöstrand *et al.*, Comput. Phys. Commun. **135**, 238 (2001).
[21] R. Brun and F. Carminati, CERN Program Library Long Writeup W5013, 1993 (unpublished).
[22] The lightest neutralino mass for this SUSY point is ≈140 GeV and the second neutralino and the chargino masses are both ≈265 GeV; B.C. Allanach *et al.*, Eur. Phys. J. C **25**, 113 (2002).
[23] V. M. Abazov *et al.* (D0 Collaboration), Phys. Rev. Lett. **103**, 061801 (2009).
[24] W. Fisher, FERMILAB-TM-2386-E.
[25] T. Junk, Nucl. Instrum. Methods Phys. Res. A **434**, 435 (1999); A. Read, J. Phys. G **28**, 2693 (2002).